INTEGRATION, the VLSI journal 50 (2015) 39–47

Contents lists available at ScienceDirect

INTEGRATION, the VLSI journal

journal homepage: www.elsevier.com/locate/vlsi

Impact of scaling on the soft error sensitivity of bulk, FDSOI and FinFET technologies due to atmospheric radiation

G. Hubert [a,*], L. Artola [a], D. Regis [b]

[a] The French Aerospace Lab. (ONERA), Toulouse, France
[b] Thales Avionics, Le Haillan, France

ARTICLE INFO

Article history:
Received 27 May 2014
Received in revised form
15 January 2015
Accepted 15 January 2015
Available online 22 January 2015

Keywords:
Atmospheric radiation
VLSI trend
Soft error
MUSCA SEP3
FinFET
FDSOI

ABSTRACT

This paper investigates the impact of terrestrial radiation on soft error (SE) sensitivity along the very large-scale integration (VLSI) roadmap of bulk, FDSOI and finFET nano-scale technologies using the MUSCA SEP3 tool. The terrestrial radiation considered in this work includes neutron, proton, and muon particles and alpha-emitters.

The results indicate that protons and muons must be taken into account for ground environments. However, significant differences were observed for bulk, FDSOI and FinFET technologies. The down-scaling induces an increase in SEU susceptibility to radiation. An overall analysis indicates that the SER does not increase drastically with technological integration for the three technologies considered. Moreover, the results show that FDSOI and FinFET technologies provide resistance to the ionizing radiation effects due to narrow sensitivity volumes. At the ground altitudes, the total SER ranges from 10^3 and 10^4 FIT/Mbit for the planar bulk technology while it ranges from 10^2 and 10^3 FIT/Mbit for the FDSOI and FinFET technologies.

The results of analyses show that for the avionic altitude, neutron and/or the proton environments induce the main contribution to the total SER, whereas muon and α-SER impacts are negligible. For the 45-nm technological node (all types), the neutron contribution is around 60–70% of the total SER. Concerning the ground altitude, α-SER is the main contribution down to the 28-nm node. Moreover, the results suggest muon-induced upset affects the soft error rate from 32-nm SRAM operated at a nominal supply voltage and has a significant impact for circuits fabricated in smaller process technologies (22-nm and 14-nm). In addition, the results show that the muon impact can be the main contribution at 22-nm and beyond. Future terrestrial error rate predictions will require characterizations of the linear energy transfer (LET) threshold with consideration of muon and/or proton environments.

1. Introduction

When primary cosmic rays penetrate Earth's atmosphere, they interact with atmospheric nuclei and induce nuclear reactions generating secondary radiation of every type [1,2]. Products of the cosmic-ray showers are protons, electrons, neutrons, heavy ions, muons, and pions. The type of secondary radiation and its intensity depend on the altitude, the geomagnetic latitude and the Sun's activity. Neutrons are measurable at 330 km altitude, and their density increases with decreasing altitude until they reach a peak at approximately 20 km. At sea level, muons [3, 33, 39] are the most numerous terrestrial species. Muons are decay products of mesons produced in hadronic cascades (i.e., secondary particles of protons, muons or neutrons induced by a primary particle) initiated by primary cosmic rays, usually made of highly energetic protons. Secondary radiation and its intensity depend on the altitude, the geomagnetic latitude and the Sun's activity.

The radiation-induced Single Event Effect (SEE) has been identified as a major reliability issue for commercial electronic systems [1]. These perturbations, gathered under the acronym SEE are the consequence of a current pulse generated by the impact of energetic particles (heavy ions, protons, neutrons, muons, etc.) in sensitive electrodes of the circuit. Soft errors (SEs), caused mainly by cosmic rays and alpha particles induced by natural alpha emitters from materials, are increasingly affecting electronic systems, including circuits from advanced CMOS technologies, as the process node scales down. SEs, which began to appear at the end of the 1960s for space applications, currently constitute a major challenge, not only for embedded systems of space and avionic applications but also for any system operating at the ground level for which a fault may have critical consequences.

The constant progress in integrated circuit manufacturing technologies have resulted in significant reductions of transistor

* Corresponding author.

http://dx.doi.org/10.1016/j.vlsi.2015.01.003
0167-9260/

dimensions. This makes very large-scale integration (VLSI) circuits increasingly sensitive to perturbations due to the effects of natural radiation present in the environments where they operate.

With continued advancements in process manufacturing technology, a set of new error mechanisms has been developed. With such advanced technologies, the track effect, i.e., the radial ionization profile, is expected to be critical [14] with multiple-cell upsets (MCUs) acting as the main contributor [15–17]. As feature sizes scale down, charge collection at multiple nodes (i.e., charge sharing) due to a single particle hit result from the decrease in spacing dimensions between cells [4–7]. The sensitivity of the SEE is expected to increase and recent studies have demonstrated the occurrence of SEs due to protons [8,9] and muons [10] for advanced nano-scale electronics.

SEE modeling applied to nano-scale technologies is still a challenge. In the past ten years, multi-physics modeling based on Monte-Carlo simulations have been developed [13, 18–22] to overcome the obsolescence of engineering models at predicting SEE rates (SERs). These new methods are essential to evaluate the device sensitivity and to investigate evolving technologies and observe emerging SEE mechanisms. Multi-physics approaches allow modeling of the radiation field (including complex radiation fields), the transport of primary particles in the sensitive target throughout the overall shielding, package and back end of line (BEOL), the generation of electron–hole pairs in the semiconductor via direct or indirect ionization mechanisms, the charge transport and collection, and the circuit electrical response.

MUSCA SEP3 (MUlti-SCAles Single Event Phenomena Predictive Platform, [22]), in development at ONERA since 2007, consists of sequentially modeling the physical and electrical mechanisms involved in the SEE occurrence, from the system level down to the semiconductor target. Investigations were performed and validated in several scientific fields, such as operational calculations [23,24], nano-scale technologies (bulk, FDSOI [10] and FinFET [25]) and the design impact on SEE responses [26], transport/collection models [27] and emerging problematic issues (direct ionizing protons [9] and muons). Significant works have additionally investigated the contribution of the radial ionization profile of SEE modeling [10–12].

Based on the ability of MUSCA SEP3 to model SEs in nanometric devices [25,27,28], this paper investigates the terrestrial radiation impacts on the SEU sensitivity along the scaling trend of FDSOI and bulk CMOS nano-scale technologies. Radiation fields considered in this work include neutrons, protons, muons and alpha-emitters.

2. SEE multi-physics modeling for advanced VLSI technologies

2.1. MUSCA SEP3 description

MUSCA SEP3 was fully presented in previous works [22,28]. It consists of modeling the whole device within its local and global environments, and the detailed characteristics of the radiation field environment (nature, direction and spectrum).

The results presented in 2009 have shown that each physical level is critical for the SEE risk calculation including the environment description. Fig. 1 describes the MUSCA SEP3 platform, which allows for the calculation of the SEU sensitivity and characteristics.

In the framework of this study, MUSCA SEP3 is used to model the nano-scale FDSOI and bulk CMOS technologies, considering the atmospheric radiation fields. Thus, three main problems can be taken into account: first, defining neutron, proton and muon environments; second, modeling the interactions of particles in Silicon including the radial distribution of deposited charges; third, modeling the transport-collection mechanisms for nano-scale technologies.

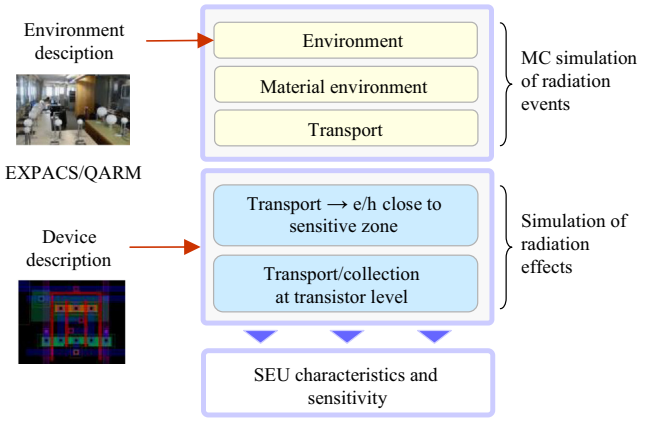

Fig. 1. Global methodology applied in this work and used in MUSCA SEP3 platform.

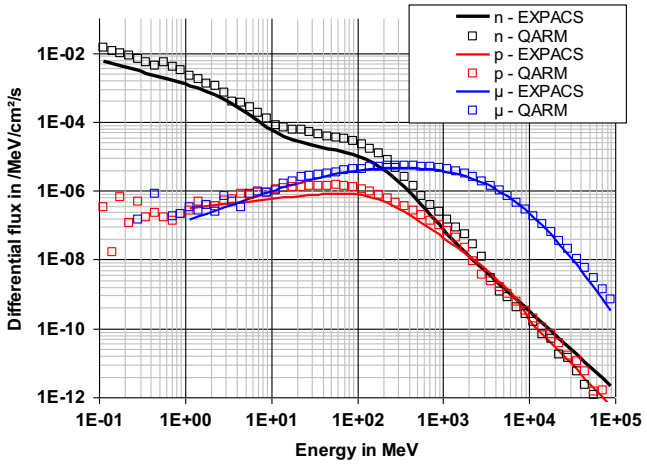

Fig. 2. Neutron, proton and muon spectra from EXPACS [30] and QARM [29] tools considering ground altitude and the Toulouse location (43 °36′16″ North, 1 °26′38″ East).

2.2. Radiation field modeling

The first step consists of modeling the radiation fields, i.e., atmospheric neutron, proton, and muon environments. The atmospheric radiation can be deduced from tools such as QARM [29] and EXPACS [30]. The QARM tool is based on databases containing the response of the atmosphere to incident particles of the upper atmosphere, which are calculated using Monte-Carlo simulations (GEANT4) of particle transport through the atmosphere. The EXPACS tool is based on analytical functions deduced from the PHITS code (Monte-Carlo simulations using JENDL-High energy model) [31].

Fig. 2 presents the spectrum (n° i.e., neutron, p^+ i.e., proton and μ i.e., muon) calculated for the ground altitude, considering the Toulouse location (43 °36′16″ North, 1 °26′38″ East). The results include data from EXPACS [30] and QARM [29]. The neutron, proton and muon fluxes are equal to 1×10^{-2}, 5.8×10^{-4}, 2.2×10^{-2} particles/cm²/s, respectively. These results confirm that muons are the most numerous terrestrial species at the ground level. Nevertheless, the results from both tools are similar. The angular properties can be taken into account. The QARM tool provides these properties as it allows for distinguishing the upward and downward neutron/proton and muon fluxes. The muon field model considers an angular distribution defined by

$\cos^2(\theta)$, where θ is the zenith angle (the angle between the direction of interest and the local zenith) [3].

In this work, the SEE includes the neutron and proton effects, but it is necessary to take into account the emitter alpha contribution. Alpha-emitting impurities can be found in some packaging materials, chemicals and materials used in the chip fabrication process. The emission rate can strongly vary depending on the quantity and purification grade of these materials. MUSCA SEP3 has therefore been adapted to investigate and quantify the α-SER contribution; however, the material properties required to define the alpha-emissivity types and their locations are rarely available. The α-emitter contamination effect is considered here to be the sum of the package and wafer contributions. The alpha emissions are considered isotropic and locations are randomly chosen. Four alpha emission categories can be considered for the package: the hyper-low-alpha (HLA, $\varepsilon < 5 \times 10^{-4}$ α/cm²/h), the ultra-low-alpha (ULA, $\varepsilon < 10^{-3}$ α/cm²/h), the low-alpha (LA, $\varepsilon < 10^{-2}$ α/cm²/h) and the standard (S, $\varepsilon \sim 10$ to 10^{-2} α/cm²/h). In this work, we consider a uniform alpha-emissivity rate equal to 5×10^{-4} alpha/cm²/h (HLA); the alpha emissivity induced by wafer contamination is typically much lower [32–34].

2.3. Interaction of radiations with silicon

As mentioned previously, the interactions of radiation with silicon integrated circuits contribute to SEEs when ionizing devices along the primary or secondary particle path. Indeed, neutrons and protons can interact with the nucleus either by elastic and non-elastic interactions and transfer a significant part of their energies to the recoil. Secondary ions produced in an interaction extend from a proton (or neutron) to the nucleus of the target atom. Thus, secondary ions lose their energies by coulomb interaction with the electrons of the target atoms, and at the end of their range, by elastic collisions with the atoms. In Silicon, secondary ions created by nuclear interactions can range from H to P (capture reaction), including several isotopes. Moreover, a nuclear reaction is likely to induce several secondary ions.

In MUSCA SEP3, nuclear databases have been developed using GEANT4 [37] for atomic species including Si, O, Cu and W with neutrons and protons. Databases provide secondary ion counts, atomic and mass numbers, their energies and directions. The GEANT4.9.0.p01 version of GEANT4 with the pre-compound+Binary cascade model for inelastic nuclear interaction and the standard nuclear elastic model for elastic interactions have been used. A second database has been generated with SRIM [38] that contains the LET and Range characteristics. The muon characteristics (i.e., LET and Range) are deduced from the Bethe-Block equations. Fig. 3 shows the muons and protons range and LET in Silicon as a function of energy.

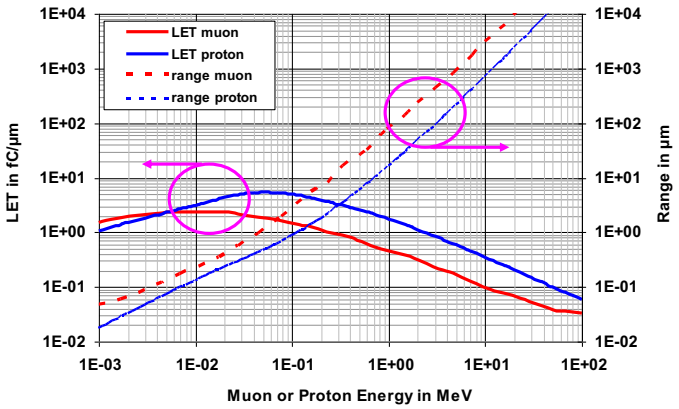

Fig. 3. LET and range characteristics in Silicon for protons and muons.

With continued advancements in process manufacturing technology, the radial profile of deposited charges induced by primary or secondary particles (including ions and muons) can be comparable to the topology of several cells. Thus, knowledge of the electron–hole pair density in the ion track is necessary for estimating device reliability of nano-scale transistors. Generally, a Gaussian shape can be considered. Recent works [10–12] based on GEANT4 calculations show the increasing importance of taking into account the radial distribution of deposited charges with technology integration, to accurately predict the SEE sensitivity. To predict SEE in future scaled technologies, the ability to describe extreme events and potential (but rare) multiple bit upsets (MBU) with high multiplicity will be required, particularly for advanced technology nodes, where complex sensitivity volumes will appear.

Thus, an important challenge is the treatment of the very small volumes of the active silicon volume, in particular, the processes of energy deposition (i.e., the distribution of particle energies in a given environment). The ion-tracks and muon-tracks are simulated in silicon with GEANT4 to quantify the radial profile parameters of the deposited charge. Thus, MUSCA SEP3 is able to model the radiation fields composed by neutrons, protons and muons and to take into account the energy depositions in silicon taking into account their 3D tack morphologies.

2.4. FDSOI and bulk nano-scale technology modeling

Technology advancement has been followed by lowering operating voltage, lowering nodal capacitance and increasing the integration density. Moreover, the trend also has taken advantage of device engineering from various aspects, for example 2D as compared to 3D devices such as multigate FinFET transistors, and device structure such as bulk as compared to SOI transistor. In this study the inverter circuits in three technologies are considered: bulk CMOS, bulk FinFET and FDSOI transistor (see Fig. 4).

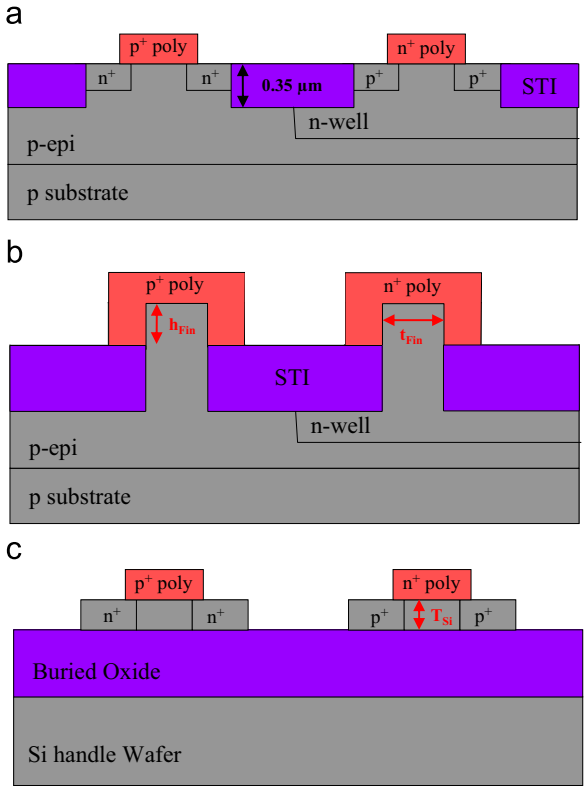

Fig. 4. Cross-section of technologies considered in this work: (a) bulk planar MOS transistor, (b) bulk FinFET and (c) FDSOI transistor.

The collection depth decreases with the integration and varies according to the technology (the well depth and the raised SOI junction for bulk and SOI, respectively). The key dimensional parameters are the height and thickness of the Fin for the FinFET technology, whereas the active silicon thickness T_{Si} is the main parameters for the SOI technology.

Concerning the SOI technologies, the main advantages are the suppression of the parasitic thyristor inducing latchup and the small silicon volume limited by the buried oxide. The deposited charge can also be amplified by the bipolar amplification mechanism.

The parasitic NPN bipolar transistor of the NMOS may be switched on by the ion. As the limited silicon layer increases the base resistance, the emitter-base voltage may increase due to holes remaining in the base, and the emitter-base junction (source-substrate) may become forward biased. The contribution of the electron current injected by the emitter in the NMOS will then be added to the ion primary photocurrent. The resulting amplification by the parasitic bipolar depends on the distance of the injected charge to the base region (under the gate), where the bipolar is the most efficient.

This phenomenon is specific to partially depleted SOI (PDSOI) devices but also exists in FDSOI. The bipolar amplification is a main key-parameter that characterizes the device sensitivity. Previous works based on experiments and TCAD investigations indicate that the bipolar effect mainly concerns the gate region. Thus, for the SOI structure, the sensitive surface can be reduced to the gate region while significant charge is collected on the drain surface area for the bulk transistor. The bipolar effect depends on the doping profiles, the technological node and the deposited charge density (i.e., the LET).

Thus, Table 1 describes the main technological model parameters [35,36]: (1) S_{cell}, Q_{crit} and V_{dd}, (2) the active silicon thickness T_{Si} for FDSOI technologies and (3) the height (h_{Fin}) and the thickness (t_{Fin}) of the Fin for the FinFET technology. The FinFET model considers one Fin per transistor. Each device type was characterized by similar specifications (i.e., V_{th}, I_{on}, S_{cell}, Q_{crit} and V_{dd}).

To complete the technological model, a structure extraction methodology based on ITRS or GDS analyses allows for deducing device descriptions including the drain/source topologies for NMOS and PMOS transistors, well dimensions, cell spacing, STI, etc. Primary or secondary ion transport in the substrate module involves the modeling of electron–hole pair generation in the semiconductor as well as drift, diffusion, collection and recombination processes. Other parasitic phenomenon such as bipolar amplification may also be considered. Charge transport in the semiconductor lattice is prone to diffusion induced by the carrier concentration gradient and drift induced by the electric field. The transport/collection physical models are based on diffusion properties and collection mechanisms studied using TCAD simulations, which aim at identifying the physical mechanisms and technological or design impacts. The main improvement consists of taking into account the dynamic coupled ambipolar diffusion and collection velocity. The approach is based on charge sharing rules, which depend on the distance from the strike location to the collection volume, the local electric field, and the process parameters (substrate/well doping).

To describe the current waveform induced by the particle, most event-rate simulators use a double exponential, based on fitting parameters obtained from TCAD simulations for a specific ion track location. Requirements of transient pulse simulation consist of linking the technology, transport/collection properties and ion characteristics.

Transient current models are based on the modeling of the successive mechanisms that occur between the entrance of a particle into matter and the SEE occurrence. Previous work [28,29] based-on TCAD investigations identify the main physical mechanisms and propose transient models based on the underlying physics phenomena (field modulation, multiple-node charge collection, and ambipolar diffusion). The complete mathematical model of the transient current is described in [28,29].

Table 1
Main technological parameters.

nm	Bulk, FDSOI and FinFET			FDSOI	FinFET	
	S_{cell} (μm²)	Q_{crit} (fC)	V_{dd} (V)	T_{Si} (nm)	h_{Fin} (nm)	t_{Fin} (nm)
65	0.55	0.6	0.9	0.9	65	40
45	0.4	0.4	0.85	0.85	45	30
32	0.25	0.3	0.8	0.8	32	25
28	0.2	0.2	0.7	0.7	28	20
22	0.15	0.12	0.7	0.7	22	15
14	0.1	0.08	0.5	0.5	14	10

3. Results and analyses for terrestrial environments

3.1. Particle-induced SEU versus the scaling trend

Fig. 5 presents the SER as a function of technological scaling for bulk CMOS (a), FDSOI (b) and FinFET (c) technologies considering the ground altitude (Toulouse location, 43 °36′16″ North and 1 °26′38″ East). The results are presented in failure-in-time (FIT) per megabit unit; one FIT equals one failure per billion (10^9) hours and is statistically projected from the results of accelerated test procedures.

The downscaling induces an increase in SEU susceptibility to radiation. An overall analysis indicates that the SER does not increase drastically with technological integration for the three technologies considered. Moreover, the results show that FDSOI and FinFET technologies provide resistance to ionizing radiation effects due to narrow sensitivity volumes.

For planar bulk technologies, α-SER (Ultra Low Alpha, i.e., $\alpha < 10^{-3}$ α/cm²/h) is the main contribution, with up to 28-nm orders of magnitude, consistent with underground experiments [40]. Moreover, the results suggest muon-induced upset affects the SER of 32-nm SRAM memory operated at a nominal supply voltage and has a significant impact for circuits fabricated in smaller process technologies (22-nm and 14-nm). In addition, the results show that muon-induced SEU becomes the main contribution at 22-nm memory and beyond.

For FDSOI technologies, the muon contribution to SER is very low. It seems that the muon SEU sensitivities in FDSOI devices are not critical for ground applications. In addition, the results suggest that muons do not affect the 14-nm technology. T_{Si} (Table 1) drastically reduces the deposited charge in the sensitivity volume. Thus, the SEU occurs for the high zenith angle.

For bulk FinFET technologies, α-SER is the main contribution up to 28-nm and proton-induced SEU becomes the main contribution from the 22-nm node and beyond. Nevertheless, muon-induced SEU is a significant contribution to SER. In fact, FinFET technologies benefit from sensitive volume sizes, but the bulk process induces diffusion mechanisms that allow the accumulation of additional charges. Complementary analyses reveal that differences observed between FDSOI and FinFET technologies are mainly induced by the direction properties of muons. Indeed, the muon field model considers an angular distribution defined by $\cos^2(\theta)$, and this is favorable and unfavorable for FDSOI and FinFET, respectively (from the point of view of SEU sensitivity).

A synthesis of the SEU risk assessment applied to scaling bulk, FDSOI and planar FinFET CMOS trends for ground environments are presented in Fig. 6. Although only protons/neutrons must be

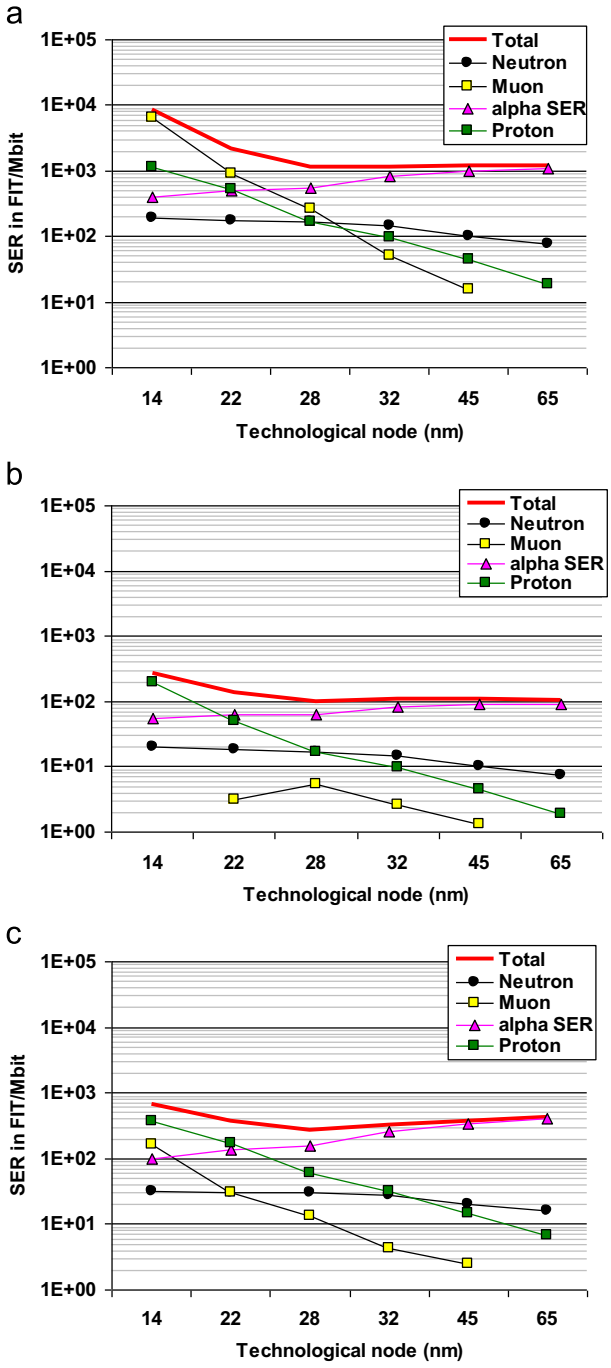

Fig. 5. SER trends for (a) bulk, (b) FDSOI and (c) FinFET technologies.

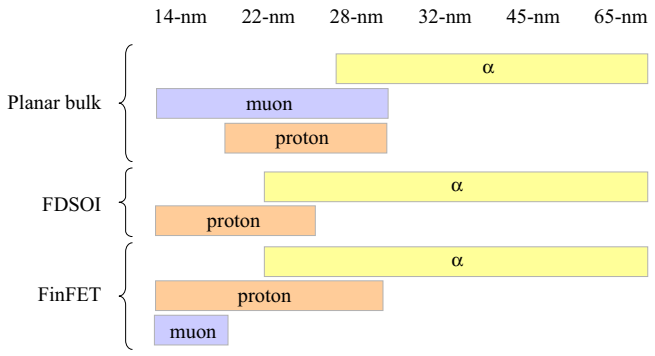

Fig. 6. SEU risk assessment applied to scaling bulk, FDSOI and FinFET CMOS trends for ground environments.

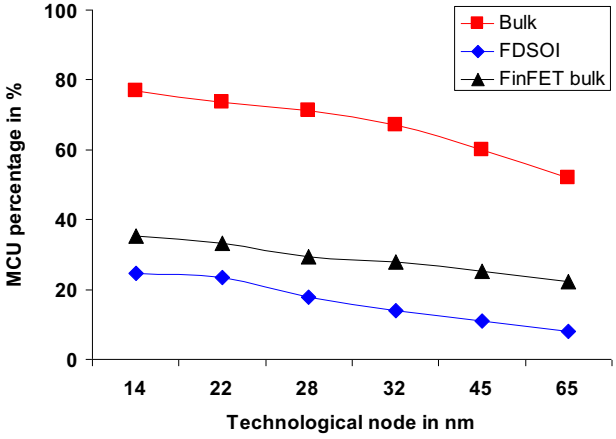

Fig. 7. MCU percentage of SER for Planar, FDSOI and FinFET technologies.

taken into account for avionic environments, muons are critical for terrestrial applications for bulk technologies (including planar and FinFET). Thus, nanometric technologies may become sensitive to the low-energy muon and/or proton spectra. Future terrestrial error rate predictions will require the characterization of the device LET threshold, consideration of the muon environment (bulk, FinFET bulk) or the proton environment (FDSOI and FinFET bulk), and advanced radiation transport computations.

3.2. *Multiple cell upset sensitivity evolution with device scaling*

With the decrease of the size of electronic devices, it is necessary to investigate multiple-cell upsets (MCU) that may potentially occur in advanced devices. Fig. 7 presents the simulated MCU ratios (in percentage) for total SEU rate as a function of the technological node and for the bulk CMOS, FDSOI and FinFET bulk technologies.

The MCU proportions increase with downscaling, and Fig. 7 shows that the FDSOI and FinFET are less sensitive to MCU than the bulk CMOS technology. FDSOI and FinFET technologies provide resistance to multiple effects thanks to their extreme limited volume sizes.

3.3. *Muon-induced SEU versus the scaling trend*

It is interesting to investigate specifically the muon contribution because the results presented in Fig. 6 indicate the critical impact of muons. Fig. 8 presents the muon contribution to SER for Bulk, FDSOI and FinFET technologies. It is also interesting to note that the muon impact is very low for FDSOI in the case of low sensitivity.

To complete this analysis, Fig. 9 presents the muon contribution to SER versus (a) the surface cell for planar bulk, (b) the active silicon thickness for FDSOI and (c) the Fin thickness for FinFET technologies.

The results consider the critical charge value presented in Table 1 (i.e., the medium value) and high and low sensitivities corresponding to *Qcrit/2* and *2xQcrit*, respectively. The results show that technological and circuit parameters (topology, bulk/FDSOI/FinFET, V_{dd}, Q_{crit} etc.) significantly impact the SEU risk induced by muons.

4. SEU trends versus the altitude effect

As presented previously, the atmospheric radiation is deduced from QARM or EXPACS. This part is devoted to investigating the

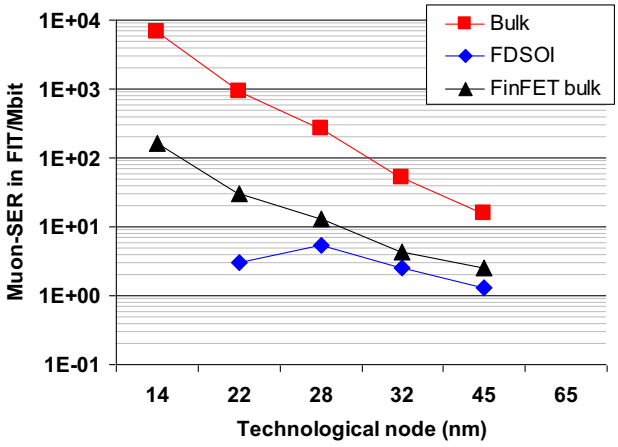

Fig. 8. Muon contribution to SER versus technological node for (a) Bulk, (b) FDSOI and FinFET technologies.

SEU trends considering altitude in the 0–15 km range. As a summary, the next figures present the SER contributions induced by neutrons, protons, α-emitter contamination and muons as a function of altitude. Fig. 10 presents SEU rates obtained for the 45-nm technological node versus altitude distinguishing the muon, proton, neutron and alpha contributions. Fig. 10(a), (b) and (c) show the bulk, the FDSOI and FinFET technologies, respectively. The results obtained for 45-nm show that the alpha contribution dominates the SER at low altitudes (<2–3 km), whereas the neutron contribution dominates at high altitudes (i.e., avionic). However, the contribution induced by protons is significant for the three technologies, and particularly for the FinFETs.

The results obtained for the 14-nm technologies are presented in Fig. 11. They show that muons are an issue for bulk technologies (planar and FinFET) operating at low altitudes (0–3 km), whereas protons are the main contributor to SER at high altitudes. The alpha emitter issue disappears for this technological scale considering HLA conditions (5×10^{-4} alpha/cm²/h).

To summarize, for the avionic altitude, neutron and/or the proton environments induce the main contribution to the total SER, whereas muon and α-SER impacts are negligible. Classically, proton direct ionization is not considered as a source of the single event effect for avionic applications. Complementary analyses based on our results show that the proton environmental impact (i.e., the direct ionization impact) is not negligible until 65-nm and becomes the main contribution from the 28-nm node and beyond. Previous works emphasize that the technological integration for over 90-nm induces an SER saturation or even slight reduction coupled with an increase of the multiple event rates. However, accounting for the direct proton ionization contribution leads to an expected strong increase in SER at 28-nm and beyond.

Concerning the ground altitude, α-SER is the main contribution down to the 28-nm node. The α-SER contribution is by far the most important compared to the neutron, proton and muon contributions, considering an Ultra Low package. Thus, it is clear that the direct ionization of proton and muon SEU sensitivities is not a critical issue for ground applications to date. Moreover, the results suggest that muon-induced upset does affect the SER from 32-nm SRAM operated at a nominal supply voltage and has a significant impact for circuits fabricated in smaller process technologies (22-nm and 14-nm). In addition, the results show that the muon impact can be the main contribution at 22-nm and beyond.

To induce an SEU by direct ionization, the Bragg peak must be localized in the sensitive region of the device. Therefore, accounting the local and global environments of the target in its operational configuration (structure, package, and device, including metallization,

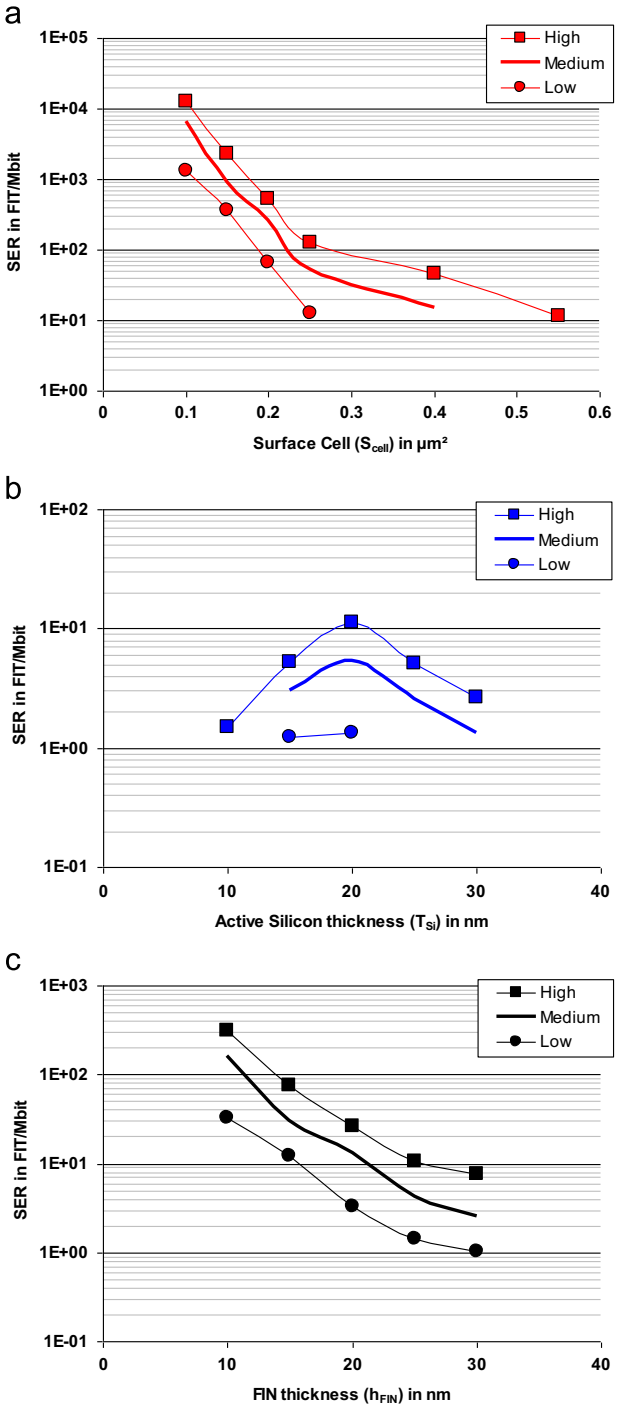

Fig. 9. Muon contribution to SER: (a) versus the surface cell for planar bulk, (b) versus the active silicon thickness for FDSOI and (c) versus the Fin thickness for FinFET technologies. The results consider the critical charge value presented in Table 1 (medium value), and high and low sensitivities corresponding, respectively to *Qcrit/2* and *2xQcrit*.

passivation and semiconductor layers) only a specific energy range is able to meet this condition. Considering the muon direction properties, the angle of incidence and the location of strike are also critical parameters to induce an SEU with this mechanism. Thus, analyses show that the low-energy muon spectrum ($\sim$10 MeV) is responsible for SEU.

Fig. 12 summarizes a risk assessment applied to scaling (a) bulk, (b) FDSOI and (c) FinFET CMOS trends versus altitude. Thus, the data

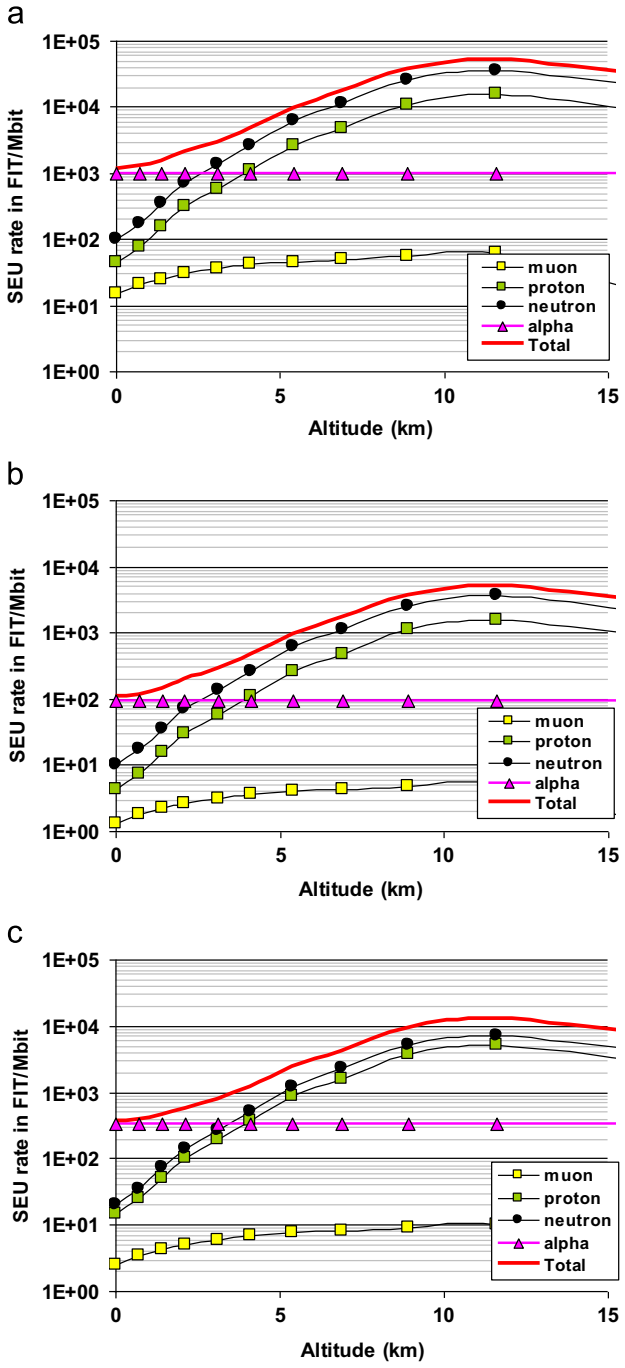

Fig. 10. SEU rate versus altitude distinguishing muon, proton, neutron and alpha contributions: (a) 45-nm bulk, (b) 45-nm FDSOI and (c) 45-nm FinFET.

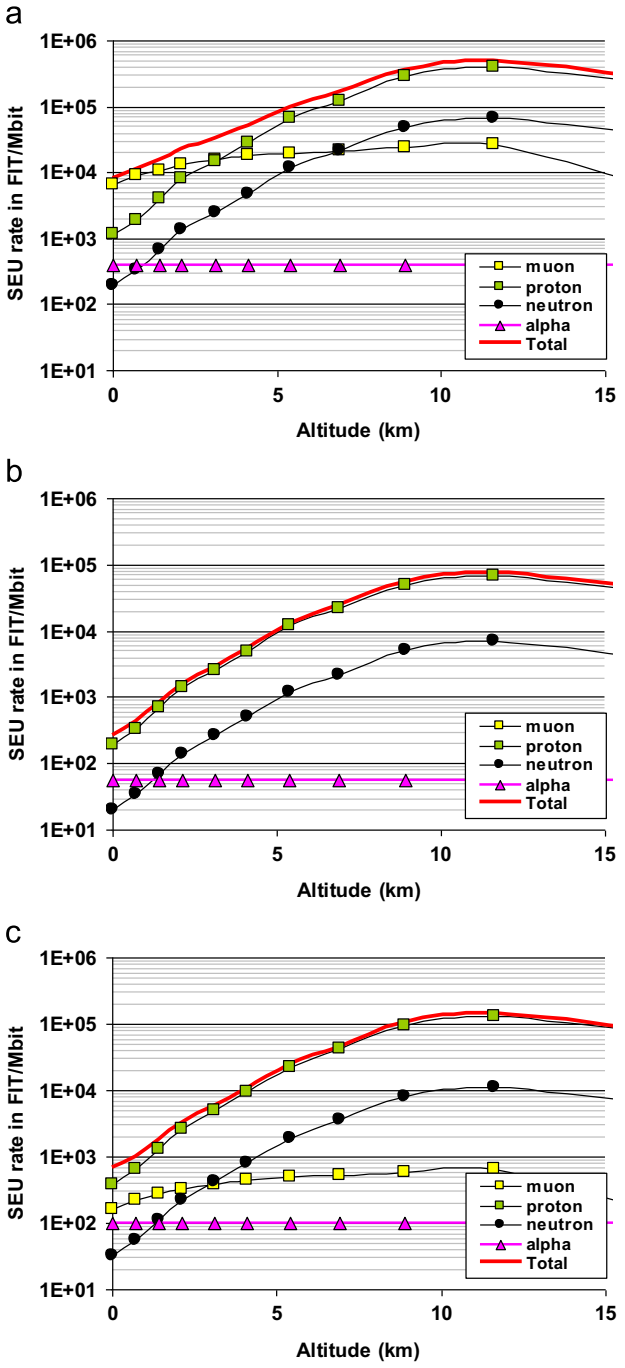

Fig. 11. SEU rate versus altitude distinguishing muon, proton, neutron and alpha contributions. The results are obtained considering SRAM devices based on (a) 14-nm bulk, (b) 14-nm FDSOI and (c) 14-nm FinFET.

presented in Fig. 12 allows for the identification of the most dangerous particle to the SER as function of the altitude and technology.

5. Conclusion

This paper proposes to model and investigate, thanks to the MUSCA SEP3 platform, the atmospheric cosmic rays impact on the SER along the scaling VLSI roadmap, including the bulk CMOS, the FDSOI and the FinFET bulk technologies. Neutron, proton, muon environments and alpha-emitters are considered.

The modeling approach considers the radiation fields from QARM and EXPACS. Moreover, an important step was to consider the very small sensitivity volumes (mainly for FinFET and FDSOI) of the active silicon volume and particularly the processes of energy deposition (i.e., distribution of particle energies in a given environment). Ion-tracks and muon-tracks in Silicon were considered with GEANT4 to quantify the radial profile parameters of the deposited charge.

The first results indicate that protons and muons must be taken into account for ground environments. However, significant differences were observed for bulk, FDSOI and FinFET technologies. Future terrestrial error rate predictions will require the characterization of the LET threshold and consideration of muon/proton

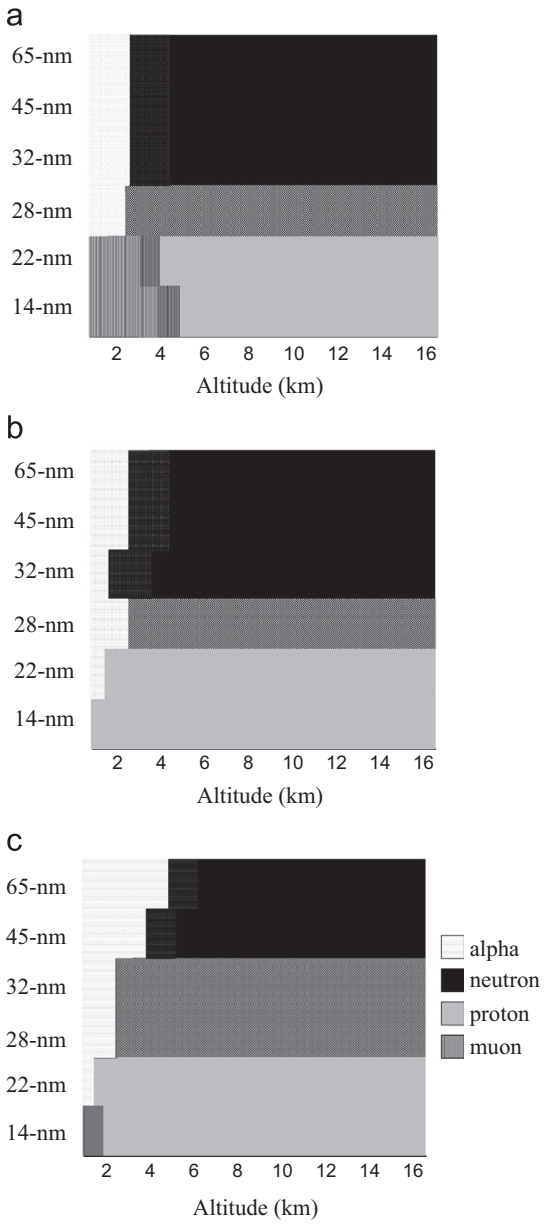

Fig. 12. Risk assessment applied to scaling (a) bulk, (b) FDSOI and (c) FinFET CMOS trends versus altitude.

environments. In addition, the mechanism for energy deposition is a main parameter to model the radiation effects on advanced devices. The results show that technological and circuit parameters (topology, bulk/FDSOI/FinFET, V_{dd}, Q_{crit} etc.) significantly impact the SEU risk induced by particles.

The results show that the downscaling induces an increase in SEU susceptibility to radiation. An overall analysis indicates that the SER does not increase drastically with the technological integration and for the three technologies considered. Moreover, the results show that FDSOI and FinFET technologies provide resistance to ionizing radiation effects due to narrow sensitivity volumes. At the ground altitudes, the total SER ranges from 10^3 and 10^4 FIT/Mbit for the planar bulk technology while it ranges from 10^2 and 10^3 FIT/Mbit for the FDSOI and FinFET technologies.

A synthesis about the SEU risk assessment applied to scaling bulk, FDSOI and planar FinFET CMOS trends for ground environments was presented. Although only protons/neutrons must be taken into account for avionic environments, muons are critical for terrestrial applications for bulk technologies (including planar and FinFET). Thus, nanometric technologies may become sensitive to the low-energy muon and/or proton spectra. Future terrestrial error rate predictions will require the characterization of the device LET threshold, consideration of the muon (bulk, FinFET bulk) or proton environment (FDSOI and FinFET bulk), and advanced radiation transport computations.

The altitude effect was investigated in the last part. For the avionic altitude, neutron and/or proton environments induce the main contribution to the total SER, whereas the muon environment and α-SER impact are negligible. For the 45-nm technological node (all types), the neutron contribution is around 60–70% of the total SER. Concerning the ground altitude, the direct ionization of protons and muons SEU sensitivities is not a critical issue for ground applications to date. Moreover, the results suggest muon-induced upset does affect the SER from 32-nm technologies and has a significant impact for circuits fabricated in smaller process technologies. In addition, the results show that the muon impact can be the main contribution for the 22-nm node and beyond.

References

[1] J.F. Ziegler, Terrestrial cosmic rays, IBM J. Res. Dev. 40 (1) (1996, 19-39).
[2] J.L. Barth, et al., Space, atmospheric, and terrestrial radiation environments, IEEE Trans. Nucl. Sci. 50 (3) (2003, 466-482).
[3] K. Nagamine, Cambridge University Press, 2003.
[4] A. Oluwole, et al., Charge collection and charge sharing in a 130 nm CMOS technology, IEEE Trans. Nucl. Sci. 53 (6) (2006) 3253–3258.
[5] B.D. Olson, et al., Analysis of parasitic bipolar transistor mitigation using well contacts in 130 nm and 90 nm CMOS technology, IEEE Trans. Nucl. Sci. 54 (4) (2007) 894–897.
[6] A.M. Francis, et al., Significance of strike model in circuit-level prediction of charge sharing upsets,, IEEE Trans. Nucl. Sci. 56 (6) (2009) 3109–3114.
[7] J.D. Black, et al., Characterizing SRAM single event upset in terms of single and multiple node charge collection, IEEE Trans. Nucl. Sci. 55 (6) (2008) 2943–2947.
[8] B.D. Sierawski, et al., Impact of low-energy proton induced upsets on test methods and rate predictions, IEEE Trans. Nucl. Sci. 56 (6) (2009) 3085–3092.
[9] G. Hubert, et al., MUSCA SEP3 contributions to investigate the direct ionization proton upset in 65 nm technology for space and atmospheric applications, in: Proceedings of the Radiation and its Effects on Components and Systems, RADECS 2009.
[10] M. Raine, et al., Impact of the radial ionization profile on SEE prediction for SOI transistors and SRAMs beyond the 32-nm technological node, IEEE Trans. Nucl. Sci. 58 (3) (2011) 840–847.
[11] M. Raine, et al., Implementing realistic heavy ion tracks in a SEE prediction tool: comparison between different approaches, IEEE Trans. Nucl. Sci. 59 (4) (2012) 950–957.
[12] M. Raine, et al., Monte-Carlo prediction of heavy ion induced MBU sensitivity for SOI SRAMs using radial ionization profile, IEEE Trans. Nucl. Sci. 58 (6) (2011) 2607–2613.
[13] R.A. Reed, et al., Impact of ion energy and species on single event effects analysis, IEEE Trans. Nucl. Sci. 54 (2007) 2312–2321.
[14] A. Akkerman, et al., Ion and electron track structure and its effects in silicon: model and calculations, Nucl. Instrum. Methods Phys. Res. B 227 (2005) 319–336.
[15] E.H. Cannon, et al., Multi-bit upsets in 65 nm SOI SRAMs, in: Proceedings of IRPS, 2008.
[16] R.K. Lawrence, et al., Single event effect induced multiple-cell upset in a commercial 90 nm CMOS digital technology, IEEE Trans. Nucl. Sci. 55 (6) (2008) 3367–3374.
[17] N. Seifert, et al., Multi-cell upset probabilities of 45 nm high-k+metal gate SRAM devices in terrestrial and space environments, in: Proceedings of IRPS, 2008, pp. 183–185.
[18] Y. Tosaka, et al., Simulation technologies for cosmic ray neutron-induced soft errors: models and simulation systems, IEEE Trans. Nucl. Sci. 46 (3) (1999) 774–780.
[19] H.H.K. Tang, et al., SEMM2: a modelling system for single event analysis, IEEE Trans. Nucl. Sci. 51 (6) (2004) 3342–3348.
[20] K.M. Warren, et al., Monte-Carlo based on-orbit single event upset rate prediction for a radiation hardened by design latch, IEEE Trans. Nucl. Sci. 54 (6) (Dec. 2007) 2419–2425.
[21] R.A. Reed, et al., Anthology of the development of radiation transport tools as applied to single event effects, IEEE Trans. Nucl. Sci. 60 (3) (2013) 1876–1911.
[22] G. Hubert, et al., Operational SER calculations on the SAC-C orbit using the Multi Scales Single Event Phenomena Predictive Platform (MUSCA SEP3), IEEE Trans. Nucl. Sci. 56 (6) (2009) 3032–3042.
[23] G. Hubert, et al., Impact of the solar flares on the SER dynamics on micro and nanometric technologies, IEEE Trans. Nucl. Sci. 57 (6) (2010).

[24] G. Hubert, et al., Operational impact of statistical properties of single event phenomena for on-orbit measurements and predictions improvement, IEEE Trans. Nucl. Sci. 60 (5, Part: 3) (2013) 3915–3923.
[25] L. Artola, et al., Modeling of radiation-induced single-event-transients in SOI FinFETs, in: Proceedings of the IEEE Reliability Physics Symposium, April 2013.
[26] G. Hubert, et al.,Single event transient analyses based on experiments and multi-physics modeling applied to the hardened ATMEL CMOS library in 180 and 90-nm technological nodes, Submitted to Nuclear Science Conference, Paris, July 2014.
[27] L. Artola, et al., SEU prediction from SET modeling using multi-node collection in bulk transistors and SRAMs down to the 65 nm technology node, IEEE Trans. Nucl. Sci. (2011, 1338-1346).
[28] G. Hubert, et al., Single-event transient modeling in a 65-nm bulk CMOS technology based-on multi-physical approach and electrical simulations, IEEE Trans. Nucl. Sci. 60 (6, Part: 1) (2013).
[29] QinetiQ Atmospheric Radiation Model, QARM, Available on ⟨http://www.qarm.eu⟩.
[30] EXPACS Homepage, ⟨www.phits.jaea.go.jp/expacs⟩.
[31] T. Sato, et al., Analytical functions to predict cosmic-ray neutron spectra in the atmosphere, Radiat. Res. 166 (2006) 544–555.
[32] R. Heald, How cosmic rays cause computer downtime, IEEE Rel. Soc. SCV Meeting, 2005.
[33] J.F. Ziegler, et al., SER—history, trends and challenges, Cypress Semiconductors, 2004.
[34] R. Baumann, et al., Call for improved ultra-low background alpha-particle emission metrology for the semiconductor industry, Int. SEMATECH Technology Transfer, 2001.
[35] B.D. Sierawki, et al., Effects of scaling on muon-induced soft errors, in: Proceedings of IRPS, 2011.
[36] International Technology Roadmap Semiconductors, ⟨www.itrs.net⟩.
[37] GEANT4 Homepage, ⟨www.geant4.web.cern.ch⟩.
[38] SRIM: ⟨http://www.srim.org/⟩, the Stopping and Range of Ions in Matter.
[39] B.D. Sierawski, et al., Muon-induced single event upsets in deep-submicron technology, IEEE Trans. Nucl. Sci. (2010, 3273-3278).
[40] A. Lesea, et al., Qualification methodology for sub-micron ICs at the low noise underground laboratory of rustrel, IEEE Trans. Nucl. Sci. (2008, 2148-2153).